THE JOURNAL OF PHYSICAL CHEMISTRY LETTERS
A JOURNAL OF THE AMERICAN CHEMICAL SOCIETY

pubs.acs.org/JPCL

Letter

Vibrational Signature of Dynamic Coupling of a Strong Hydrogen Bond

Shukang Jiang,[▽] Mingzhi Su,[▽] Shuo Yang,[▽] Chong Wang,[▽] Qian-Rui Huang,[▽] Gang Li, Hua Xie, Jiayue Yang, Guorong Wu, Weiqing Zhang, Zhaojun Zhang,* Jer-Lai Kuo,* Zhi-Feng Liu,* Dong H. Zhang, Xueming Yang, and Ling Jiang*

Cite This: *J. Phys. Chem. Lett.* 2021, 12, 2259−2265

Read Online

ACCESS | Metrics & More | Article Recommendations | Supporting Information

ABSTRACT: Elucidating the dynamic couplings of hydrogen bonds remains an important and challenging goal for spectroscopic studies of bulk systems, because their vibrational signatures are masked by the collective effects of the fluctuation of many hydrogen bonds. Here we utilize size-selected infrared spectroscopy based on a tunable vacuum ultraviolet free electron laser to unmask the vibrational signatures for the dynamic couplings in neutral trimethylamine−water and trimethylamine−methanol complexes, as microscopic models with only one single hydrogen bond holding two molecules. Surprisingly broad progression of OH stretching peaks with distinct intensity modulation over ∼700 cm^{-1} is observed for trimethylamine−water, while the dramatic reduction of this progression in the trimethylamine−methanol spectrum offers direct experimental evidence for the dynamic couplings. State-of-the-art quantum mechanical calculations reveal that such dynamic couplings are originated from strong Fermi resonance between the stretches of hydrogen-bonded OH and several motions of the solvent water/methanol, such as translation, rocking, and bending, which are significant in various solvated complexes commonly found in atmospheric and biological systems.

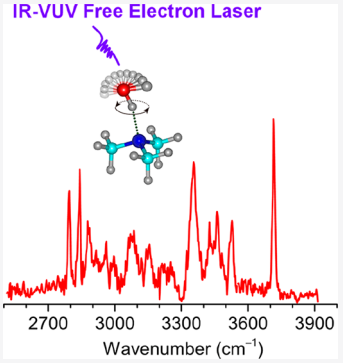

Hydrogen bonds (HBs) are the main intermolecular interactions responsible for solvation, molecular self-assembly, biological processes, and the formation of atmospheric particles.[1−5] The small mass of hydrogen means that the HBs are inherently fluctuant in nature, which play a crucial role in determining the structures, properties, and reaction dynamics.[1] What role does the solvent play in such HB fluctuations? What vibrational motions trigger these HB fluctuations? How are the HB fluctuations manifested in the vibrational spectra? Experiments to address these questions offer the opportunity to better understand the intrinsic properties of HB motions associated with proton transport in biology and atmosphere such as fuel-cell membranes and new particle formation.[5,6] However, for measurements in condense phases, the collective effects of vibrational couplings produce diffuse bands which are hard to analyze.

Mass-selected solvation clusters are molecular models which can be interrogated in the gas phase with better spectral resolution, providing microscopic details about HB fluctuations.[7−11] Large amplitude motions of multiple HBs have been characterized in a few hydrated cluster ions, such as $H_3O^+(TMA)_3$ (TMA = trimethylamine, $(CH_3)_3N$),[12] $H_3O^+(18C6)$ (18C6 = 18-crown-6 ether),[13] $NO_3^-(H_2O)_n$,[14,15] $HCO_2^-(H_2O)_n$,[15] and $H_2PO_4^-(H_2O)_n$.[16] The OH stretching (ν_{OH}) region of the HB donor is especially interesting, which could be extended over 400−800 cm^{-1}. Unfortunately, such a progression either is unresolved, as in the case of $H_3O^+(TMA)_3$ and $H_3O^+(18C6)$,[12,13] or involves the flipping of two HBs, as in the case of $NO_3^-(H_2O)$.[14,15]

Studying HBs in neutral clusters is more challenging, due to the difficulty in size selection. For small clusters, size-selective measurement can be achieved by rotationally resolved spectra, and such studies on X−H_2O complexes (X = H_2O, TMA, N_2, etc.) did provide important insights into the intermolecular forces and the complex quantum tunneling dynamics.[17−19] Yet, even for such small clusters, there are often several ways to arrange the HBs, producing multiple isomers that complicate the interpretation of the experimental spectra. Recently, we have developed a tunable vacuum ultraviolet free electron laser (VUV-FEL),[20] which makes it possible to measure the size-selected vibrational spectra of confinement-free, neutral clusters by the infrared-vacuum ultraviolet (IR-VUV) scheme, with vibrational modes excited by an IR laser and size-selective detections achieved by VUV soft ionization near the threshold.[21−23]

The subjects for this study are the neutral TMA−H_2O and TMA−CH_3OH complexes. With a large proton affinity (227

Received: January 17, 2021
Accepted: February 22, 2021
Published: February 26, 2021

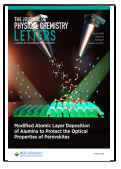

kcal/mol),[24] TMA is an acceptor for a strong HB from either H_2O or CH_3OH. The Fourier transform infrared (FT-IR) absorption spectra of a gaseous TMA−CH_3OH mixture have been measured over decades, as an archetypical model for HB interactions.[25−30] The broad OH stretching band observed previously is a clear indication of the coupling between HB fluctuation and OH stretching, but unfortunately, it was an unresolved diffuse band. The only high-resolution study on TMA−H_2O was performed in the microwave region with rotational excitations.[18] More recent interest in these complexes is due to their central role in the formation of atmospheric nanoparticles with a strong impact on human health and climate.[5,31−33] With the IR-VUV technique applied to very cold clusters in the gas phase, TMA−H_2O and TMA−CH_3OH can be viewed in a new light: two molecules held together by a single H-bond, as fundamental molecular models to probe the coupling between the vibrational excitation of a hydrogen-bonded OH bond and the fluctuation of the relevant HB. The underlying dynamics of intramolecular and intermolecular motions can now be examined in detail by both the state-of-the-art experimental and theoretical techniques.

Herein, we report the well-resolved IR spectra of mass-selected TMA−H_2O and TMA−CH_3OH complexes based on threshold photoionization using a tunable VUV-FEL. Surprisingly, broad progression of OH stretching peaks with distinct intensity modulation over ∼700 cm^{-1} is observed for TMA−H_2O, while the dramatic reduction of this progression in the TMA−CH_3OH spectrum offers direct experimental evidence for the dynamic couplings. While a qualitative understanding of these features is obtained by harmonic analysis and *ab initio* molecular dynamics (AIMD) simulations, quantum mechanical calculations on the vibration modes and frequencies reproduce the progressions and provide insights into the origin of dynamic couplings among OH stretches, OH bend overtone, intermolecular rock, and intermolecular translation.

The experimental IR spectra of TMA−H_2O and TMA−CH_3OH complexes were measured using a VUV-FEL-based IR spectroscopy apparatus (see the Supporting Information (SI) for experimental details).[21] Neutral clusters were generated by supersonic expansions of gaseous mixtures seeded in helium using a high-pressure pulsed valve that is capable of producing very cold molecular beam conditions.[34] For the IR excitation of the clusters, we used a tunable IR optical parametric oscillator/amplifier system (LaserVision). Subsequent photoionization was carried out with about a 30 ns delay with a VUV-FEL light delivered by the Dalian Coherent Light Source (DCLS) facility. IR spectra were recorded in the difference mode of operation (IR laser ON minus IR laser OFF). The normalization with the IR laser pulse energy accounted for its variations over the tuning range. IR power dependence of the signal was measured to ensure that the predissociation yield is linear with photon flux.

Figure 1 shows the experimental IR spectra of TMA−H_2O and TMA−CH_3OH. Peak positions for TMA−H_2O are listed in Table 1, and those for TMA−CH_3OH are listed in Table S1. The IR spectrum of TMA−H_2O comprises six groups of peaks (labeled A−F). The easily identifiable feature is peak A (Table 1), which is assigned to the free OH stretch of H_2O.[8,9] With one H atom of H_2O substituted by CH_3, this peak should be absent in the TMA−CH_3OH spectrum, as indeed observed. The most striking observation in this work is the IR spectrum of TMA−H_2O in the H-bonded OH stretch region (Figure 1a), which shows clear progressions of at least six peaks for H-bonded OH stretches (labeled B_1−B_6). In contrast, only two H-bonded OH stretch peaks are observed in the spectrum of TMA−CH_3OH.

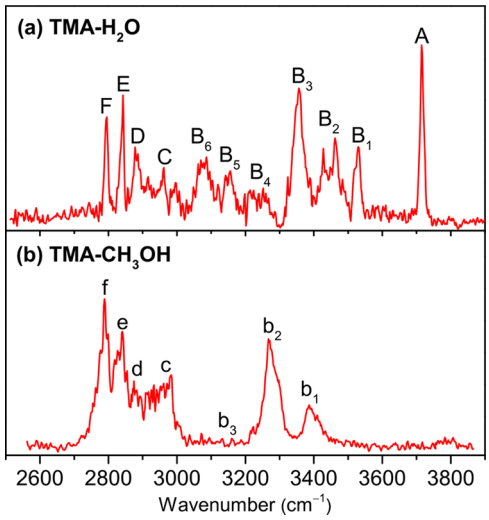

Figure 1. Experimental IR spectra of TMA−H_2O (a) and TMA−CH_3OH (b).

Table 1. Comparison of the Experimental Peak Positions (cm^{-1}) of the Neutral TMA−H_2O Complex to the Anharmonic Vibrational Frequencies Obtained from Potential-Energy-Surface Quantum Mechanical Calculations

label	exp	anharm	assignment
A	3715	3709	free OH stretch
B_1	3530	3479	coupling of water bend overtone and intermolecular translation
B_2	3462	3407	coupling among H-bonded OH stretch, water bend overtone, intermolecular translation, and intermolecular water in-plane and out-of-plane rocks
	3428	3383	
B_3	3356	3333	coupling among H-bonded OH stretch, water bend overtone, and intermolecular translation
B_4	3210	3254	coupling between H-bonded OH stretch and water bend overtone
B_5	3156	3169	coupling between H-bonded OH stretch and water bend overtone
B_6	3086	3092	coupling between H-bonded OH stretch and high-order excitation of intermolecular water out-of-plane rock
C	2992	3010	antisymmetric CH stretch
	2962	2971	
D	2885	2932	combination of two CH_3 bends
E	2842	2869	coupling of symmetric/antisymmetric CH stretches with overtones of CH_3 bend and CH_3 umbrella
F	2795	2795	coupling of symmetric CH stretch with overtones of CH_3 bend and CH_3 umbrella

To understand the experimental IR spectra and identify the structures of the TMA−H_2O and TMA−CH_3OH complexes, quantum chemical calculations and AIMD simulations were carried out (see the SI for computational details). The calculated IR spectra of TMA−H_2O and TMA−CH_3OH are compared with the experimental ones in Figure 2. In the 2700 to 3000 cm^{-1} region, sharp features labeled as C to F in the TMA−H_2O spectrum (Figure 2a) are due to CH stretching modes (ν_{CH}).[35−37] However, there are more ν_{CH} peaks than those predicted in either the harmonic (Figure 2c) or the

https://dx.doi.org/10.1021/acs.jpclett.1c00168
J. Phys. Chem. Lett. 2021, 12, 2259−2265

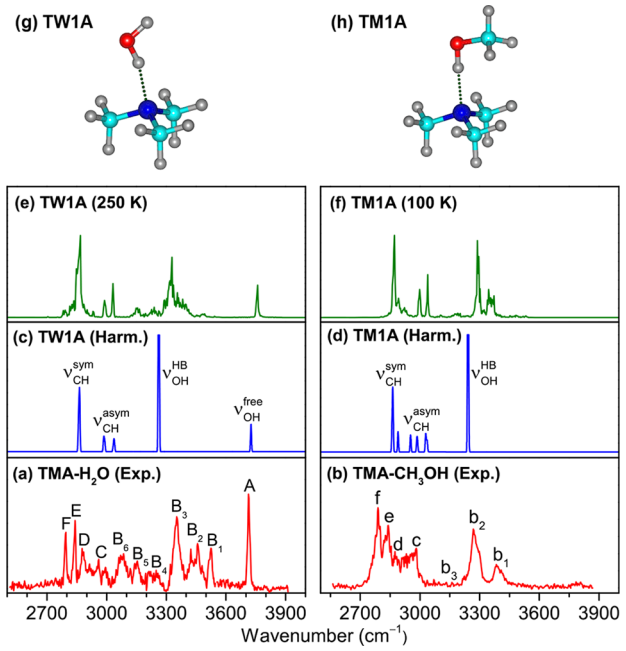

Figure 2. Comparison of the experimental and calculated IR spectra of the TMA−H_2O and TMA−CH_3OH complexes. Experimental spectra of TMA−H_2O (a) and TMA−CH_3OH (b). MP2/aug-cc-pVDZ (AVDZ) calculated harmonic vibrational spectra of global-minimum isomers TW1A (c) and TM1A (d). *Ab initio* molecular dynamic (AIMD) simulated vibrational spectra of TW1A at 250 K (e) and TM1A at 100 K (f). The corresponding structures are shown above (g and h).

AIMD spectra (Figure 2e). In the TMA−CH_3OH spectrum, the number of ν_{CH} peaks increases further, and the bands become quite congested, presumably due to the presence of an additional CH_3 group in CH_3OH.

Between 3000 and 3600 cm^{-1}, there is a progression of several broadened peaks in the TMA−H_2O spectrum (Figure 2a), although only one peak is identified in this region by the harmonic analysis (Figure 2c), which is indicated as ν_{OH}^{HB} for the hydrogen-bonded OH forming the HB with TMA. It shows the coupling between the fluctuation in the HB and the stretching of the solvated OH. Dynamic simulation by AIMD can reproduce the approximate extent of the progression (Figure 2e), as reported before,[16,38−41] and the plot of the vibrational density of states shows that features in this region are indeed due to the hydrogen-bonded OH (Figure S5). What is unique in the case of TMA−H_2O is that this progression over 600 cm^{-1} is due to the anomalously large amplitude fluctuation of a single HB.

Furthermore, the TMA−CH_3OH spectrum in the 3000−3600 cm^{-1} region offers a striking contrast with TMA−H_2O: dominated by only two peaks, b_1 and b_2, separated by only 120 cm^{-1}. CH_3OH is also bound to TMA by a single HB. With an equilibrium distance of 1.83 Å, this HB is slightly stronger than the HB in TMA−H_2O (1.86 Å). In previous studies,[16,38] it was shown that a shorter HB distance indicates stronger interactions and produces larger HB fluctuation and longer progression in the ν_{OH}^{HB} feature. Yet, the progression for ν_{OH}^{HB} in the TMA−CH_3OH spectrum is more limited than that for TMA−H_2O, indicating a significant difference in the dynamics of HB fluctuation, although neither the free H in H_2O nor the CH_3 group in CH_3OH is directly involved in the HB interactions. Moreover, it is counterintuitive that the substitution of H by a larger CH_3 group would simplify the ν_{OH}^{HB} band.

To reproduce the extent of the ν_{OH}^{HB} progression for TMA−H_2O, the AIMD simulation temperature has to be raised to 250 K (Figure S6). To do it for TMA−CH_3OH, a simulation temperature of 100 K is good enough (Figure S7). Note that AIMD treats atomic motions in classic mechanics and the simulation temperature does not really correspond to the experimental temperature, especially for cold systems, since zero-point vibrations and quantum effects are not taken into consideration,[42,43] but it does indicate the extent of atomic motions, as the temperature is calculated from the average kinetic energy.[41]

As observed in AIMD trajectories, two types of motions are involved in perturbing the single N···HO hydrogen bond holding TMA and H_2O together. The first is the stretching of this HB, and the second is the rotation of the H_2O molecule around this HB consistent with the microwave spectroscopic studies.[18] As shown in Figure 3a for TMA−H_2O, the HB bond

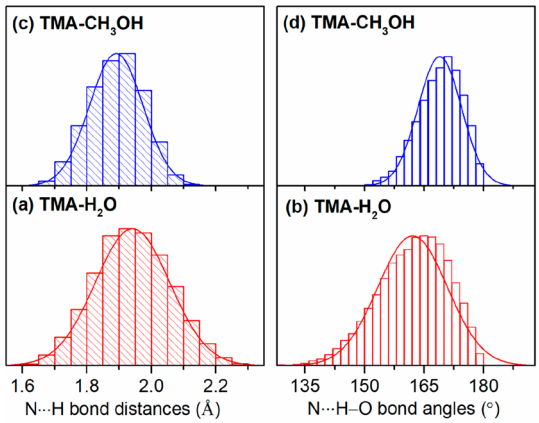

Figure 3. Normal distribution of N···H bond distances and N···H−O bond angles during AIMD simulations of TMA−H_2O at 250 K (a and b) and TMA−CH_3OH at 100 K (c and d).

distance could vary by 0.5 Å, and the N···H−O bond angle was over 50° during the AIMD run at 250 K (Figure 3b). However, these motions are much slower than the stretching of a covalent OH bond. Their effects on ν_{OH} can therefore be qualitatively examined by constraining the HB bond distance or the N···H−O bond angle to a specific value and calculating the corresponding harmonic frequencies. As shown in Figure S9a, the variation in the HB bond distance produces no obvious effect on the stretching of CH or of the free OH in the harmonic TMA−H_2O spectra. Interestingly, for ν_{OH}^{HB}, it does induce a shift of ∼600 cm^{-1} as the HB bond distance is varied from 1.72 to 2.22 Å, in the same OH stretching vibrational frequency region of the progression observed in the experimental TMA−H_2O spectrum. Similarly, such shifts could also be observed when the N···H−O bond angle is varied, although it only produces a shift over ∼300 cm^{-1} (Figure S10).

These two types of motions are also observed in the AIMD simulations for TMA−CH_3OH. As the experimental TMA−CH_3OH spectrum is best reproduced by AIMD at 100 K (Figure 2f), considerably lower than the simulation temperature of 250 K for TMA−H_2O (Figure 2e), the extent of fluctuations in the N···H bond distance and the N···H−O bond angle is less in the AIMD simulation on TMA−CH_3OH

https://dx.doi.org/10.1021/acs.jpclett.1c00168
J. Phys. Chem. Lett. 2021, 12, 2259−2265

(Figures 3c and 3d), which is responsible for the smaller frequency shifts shown in Figure S9b (and also Figure S11). Nonetheless, for the same value of the varied N···H bond distance or N···H−O angle, the calculated frequency shift in ν_{OH}^{HB} is quite similar. From the perspective of classical dynamics, the main difference between TMA−H_2O and TMA−CH_3OH is the extent of HB fluctuation. Once one H atom of H_2O is substituted by CH_3, the inertia of CH_3OH is larger than that of H_2O. Furthermore, previous experiments indicated that the barrier of internal rotation of a solvent H_2O around the HB in TMA−H_2O (∼0.003 kcal/mol) is much smaller than that of CH_3OH in TMA−CH_3OH (0.5 kcal/mol).[18,44] Going from H_2O to CH_3OH, the extent of HB fluctuation in TMA−CH_3OH is significantly reduced, compared to that in TMA−H_2O, which accounts for the observed changes in the ν_{OH}^{HB} progression of their respective spectrum.

To elucidate the origin of dynamic couplings between vibrational excitations responsible for the observed vibrational spectra, quantum mechanical treatment is needed. For that purpose, we employ two methods. For TMA−H_2O, a multidimensional *ab initio* potential energy surface (PES) is constructed by using the fundamental invariant neural network (FI-NN) fitting method (see the SI for details).[21,45−47] With the essential dimensions for the H_2O and CH_3 group included, the vibrational wave functions and frequencies are solved on such a surface. For TMA−CH_3OH, which is too large to be described by *ab initio* PES, the anharmonic vibrational spectrum of TMA−CH_3OH is calculated using the discrete variable representation (DVR) method at the CCSD/AVDZ level of theory (see the SI for details). Such a protocol has been recently applied to study the Fermi resonance in ammonia, monomethylamine, dimethylamine, and protonated trimethylamine clusters.[35,36,47−49] The calculated anharmonic vibrational spectra of TMA−H_2O and TMA−CH_3OH are compared with the experimental ones in Figure 4.

For TMA−H_2O (Figure 4c), a number of peaks are obtained with frequencies in good agreement with the experimental values. Both the ν_{OH}^{HB} and intermolecular translation play a significant role as expected, while two other modes (water bend overtone and intermolecular water rocking modes) are also involved (Table 1). The Fermi resonance between the hydrogen-bonded OH stretch and water bend overtone yields the B_4 and B_5 bands, which couples with one quantum of the translation mode to give the B_2 and B_3 bands. The splitting of band B_2 is due to the involvement of intermolecular water in-plane and out-of-plane rocks. Major contribution for the B_1 band is from the coupling of the water bend overtone and intermolecular translation. The B_6 band is mainly due to the coupling between hydrogen-bonded OH stretch and high-order excitation of intermolecular water out-of-plane rock. These results confirm the importance of the coupling between the motions of the HB (i.e., the translation, bending, or rocking of H_2O) and the stretching of hydrogen-bonded OH. As the Fermi resonance is a quantum effect, the AIMD spectrum could only produce the dynamic broadening (Figure 2e), in contrast to the splitting obtained by the anharmonic calculation.

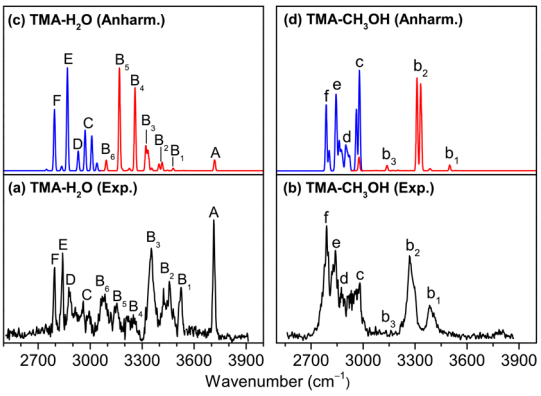

Figure 4. Comparison of the experimental and simulated anharmonic vibrational spectra of the TMA−H_2O and TMA−CH_3OH complexes. Experimental spectra of TMA−H_2O (a) and TMA−CH_3OH (b). Calculated anharmonic vibrational spectra of isomers TW1A (c) and TM1A (d). The calculated CH and OH stretching spectra are shown in blue and red, respectively. The simulated anharmonic vibrational frequencies were unscaled.

For TMA−CH_3OH (Figure 4d), the *ab initio* anharmonic calculation results confirm the significant reduction in the ν_{OH}^{HB} progression. The dominant b_2 band is due to the ν_{OH}^{HB}, and its coupling with intermolecular translation is responsible for b_1. The b_3 band is due to the coupling between the OH bend overtone and intermolecular translation. The frequency of the OH bend overtone in TMA−MeOH is lower than that in TMA−H_2O, which causes only minor intensity borrowing from the hydrogen-bonded OH stretch and produces a band at 2977 cm^{-1}. With Fermi resonance playing a less significant role, this region is better reproduced in the AIMD spectrum as shown in Figure 2f.

It is also gratifying to note that the quantum treatments also reproduce the ν_{CH} region reasonably well for both TMA−H_2O and TMA−CH_3OH. While there is little coupling between the ν_{CH} of TMA and H_2O or CH_3OH (Figure S13), there are significant couplings between CH stretches and CH_3 bends within a CH_3 group on TMA, and Fermi resonance is responsible for the extra peaks as reported recently.[35−37,49]

Note that the calculated relative intensities, especially for the ν_{OH} related features, are less satisfactory in comparison to experiment. Whether this is due to the complexity of experiment (IR absorption combined with dissociation, saturation effects, etc.) or to the limitation of theoretical calculations (neglected degrees of freedom or limited sampling of the potential energy surface, etc.) requires further studies.[23,50,51]

In summary, with TMA−H_2O and TMA−CH_3OH as archetypical models bound by a single hydrogen bond, we have been able to resolve the previously masked coupling between the fluctuation of the hydrogen bond and the stretch of hydrogen-bonded OH. The dynamic nature of such couplings is clearly demonstrated by the contrast between TMA−H_2O and TMA−CH_3OH spectra, as the substitution of H in H_2O by CH_3 significantly reduces the progression. Quantum mechanical calculations show that the more extensive splitting in the OH stretch region can be attributed to Fermi resonance, more in TMA−H_2O than in TMA−CH_3OH. The coupling between the stretch of hydrogen-bonded OH and the motion of the solvent H_2O/CH_3OH, such as translation, rocking, and bending, is an important factor in understanding these vibrational spectra. In AIMD simulations, the extent of the HB fluctuation is larger in TMA−H_2O than in TMA−CH_3OH. Such a robust hydrogen bond with a large fluctuation, as observed in the TMA−H_2O complex, has been suggested before in the water−catalyzed reactions during the formation of atmospheric new particles.[5,33] Since the proposed

https://dx.doi.org/10.1021/acs.jpclett.1c00168
J. Phys. Chem. Lett. 2021, 12, 2259−2265

vibrational coupling scheme does not rely on specific properties of TMA, the identification and understanding of such features in the TMA−H_2O and TMA−CH_3OH spectra provide a general model to elucidate the dynamic coupling of the hydrogen bond and its role in reaction mechanisms for a wide range of atmospheric and biological systems.

■ ASSOCIATED CONTENT

Supporting Information

The Supporting Information is available free of charge at https://pubs.acs.org/doi/10.1021/acs.jpclett.1c00168.

Experimental and theoretical methods; Figures S1, S2, S4−S7, and S9−S13, spectra; Figure S3, optimized structures; Figure S8, bond distances and angles; Tables S1 and S2, vibration frequences; Table S3, Cartesian coordinates; and references (PDF)

■ AUTHOR INFORMATION

Corresponding Authors

Zhaojun Zhang − *State Key Laboratory of Molecular Reaction Dynamics, Dalian Institute of Chemical Physics, Chinese Academy of Sciences, Dalian 116023, China;* orcid.org/0000-0002-4263-1789; Email: zhangzhj@dicp.ac.cn

Jer-Lai Kuo − *Institute of Atomic and Molecular Sciences, Academia Sinica, Taipei 10617, Taiwan;* orcid.org/0000-0002-0550-0181; Email: jlkuo@pub.iams.sinica.edu.tw

Zhi-Feng Liu − *Department of Chemistry and Centre for Scientific Modeling and Computation, Chinese University of Hong Kong, Shatin, Hong Kong, China; CUHK Shenzhen Research Institute, Shenzhen 518507, China;* orcid.org/0000-0002-6898-075X; Email: zfliu@cuhk.edu.hk

Ling Jiang − *State Key Laboratory of Molecular Reaction Dynamics, Dalian Institute of Chemical Physics, Chinese Academy of Sciences, Dalian 116023, China;* orcid.org/0000-0002-8485-8893; Email: ljiang@dicp.ac.cn

Authors

Shukang Jiang − *State Key Laboratory of Molecular Reaction Dynamics, Dalian Institute of Chemical Physics, Chinese Academy of Sciences, Dalian 116023, China*

Mingzhi Su − *State Key Laboratory of Molecular Reaction Dynamics, Dalian Institute of Chemical Physics, Chinese Academy of Sciences, Dalian 116023, China; University of Chinese Academy of Sciences, Beijing 100049, China*

Shuo Yang − *State Key Laboratory of Molecular Reaction Dynamics, Dalian Institute of Chemical Physics, Chinese Academy of Sciences, Dalian 116023, China; University of Chinese Academy of Sciences, Beijing 100049, China*

Chong Wang − *State Key Laboratory of Molecular Reaction Dynamics, Dalian Institute of Chemical Physics, Chinese Academy of Sciences, Dalian 116023, China; University of Chinese Academy of Sciences, Beijing 100049, China*

Qian-Rui Huang − *Institute of Atomic and Molecular Sciences, Academia Sinica, Taipei 10617, Taiwan*

Gang Li − *State Key Laboratory of Molecular Reaction Dynamics, Dalian Institute of Chemical Physics, Chinese Academy of Sciences, Dalian 116023, China*

Hua Xie − *State Key Laboratory of Molecular Reaction Dynamics, Dalian Institute of Chemical Physics, Chinese Academy of Sciences, Dalian 116023, China;* orcid.org/0000-0003-2091-6457

Jiayue Yang − *State Key Laboratory of Molecular Reaction Dynamics, Dalian Institute of Chemical Physics, Chinese Academy of Sciences, Dalian 116023, China*

Guorong Wu − *State Key Laboratory of Molecular Reaction Dynamics, Dalian Institute of Chemical Physics, Chinese Academy of Sciences, Dalian 116023, China;* orcid.org/0000-0002-0212-183X

Weiqing Zhang − *State Key Laboratory of Molecular Reaction Dynamics, Dalian Institute of Chemical Physics, Chinese Academy of Sciences, Dalian 116023, China*

Dong H. Zhang − *State Key Laboratory of Molecular Reaction Dynamics, Dalian Institute of Chemical Physics, Chinese Academy of Sciences, Dalian 116023, China*

Xueming Yang − *State Key Laboratory of Molecular Reaction Dynamics, Dalian Institute of Chemical Physics, Chinese Academy of Sciences, Dalian 116023, China; Department of Chemistry, Southern University of Science and Technology, Shenzhen 518055, China;* orcid.org/0000-0001-6684-9187

Complete contact information is available at: https://pubs.acs.org/10.1021/acs.jpclett.1c00168

Author Contributions

[V]S.J., M.S., S.Y., C.W., and Q.-R.H. contributed equally to this work.

Notes

The authors declare no competing financial interest.

■ ACKNOWLEDGMENTS

The authors gratefully acknowledge the DCLS for VUV-FEL beam time and the DCLS staff for support and assistance. This work was supported by the National Natural Science Foundation of China (92061203 and 21688102), the Strategic Priority Research Program of Chinese Academy of Sciences (CAS) (XDB17000000), International Partnership Program of CAS (121421KYSB20170012), CAS (GJJSTD20190002), Dalian Institute of Chemical Physics (DICP DCLS201701 and DCLS201702), the Ministry of Science and Technology of Taiwan (MOST 107-2628-M-001-002-MY4, MOST 108-2639-M-009-001-ASP, and MOST 109-2113-M-001-040), and the Academia Sinica. Q.-R.H. is supported by Academia Sinica Postdoctoral Research Fellowship. Z.-F.L. is thankful for support from the Research Grants Council of Hong Kong SAR Government through a GRF Grant (2130479).

■ REFERENCES

(1) Arunan, E.; et al. Defining the Hydrogen Bond: An Account (IUPAC Technical Report). *Pure Appl. Chem.* **2011**, *83*, 1619−1636.

(2) Dereka, B.; Yu, Q.; Lewis, N. H. C.; Carpenter, W. B.; Bowman, J. M.; Tokmakoff, A. Crossover from Hydrogen to Chemical Bonding. *Science* **2021**, *371*, 160−164.

(3) Whitesides, G. M.; Grzybowski, B. Self-Assembly at All Scales. *Science* **2002**, *295*, 2418−2421.

(4) Carcabal, P.; Jockusch, R. A.; Hunig, I.; Snoek, L. C.; Kroemer, R. T.; Davis, B. G.; Gamblin, D. P.; Compagnon, I.; Oomens, J.; Simons, J. P. Hydrogen Bonding and Cooperativity in Isolated and Hydrated Sugars: Mannose, Galactose, Glucose, and Lactose. *J. Am. Chem. Soc.* **2005**, *127*, 11414−11425.

(5) Zhang, R.; Khalizov, A.; Wang, L.; Hu, M.; Xu, W. Nucleation and Growth of Nanoparticles in the Atmosphere. *Chem. Rev.* **2012**, *112*, 1957−2011.

(6) Bonn, M.; Hunger, J. Between a Hydrogen and a Covalent Bond. *Science* **2021**, *371*, 123−124.

(7) Buck, U.; Huisken, F. Infrared Spectroscopy of Size-Selected Water and Methanol Clusters. *Chem. Rev.* **2000**, *100*, 3863−3890.
(8) Robertson, W. H.; Johnson, M. A. Molecular Aspects of Halide Ion Hydration: The Cluster Approach. *Annu. Rev. Phys. Chem.* **2003**, *54*, 173−213.
(9) Fujii, A.; Mizuse, K. Infrared Spectroscopic Studies on Hydrogen-Bonded Water Networks in Gas Phase Clusters. *Int. Rev. Phys. Chem.* **2013**, *32*, 266−307.
(10) Potapov, A.; Asselin, P. High-Resolution Jet Spectroscopy of Weakly Bound Binary Complexes Involving Water. *Int. Rev. Phys. Chem.* **2014**, *33*, 275−300.
(11) Heine, N.; Asmis, K. R. Cryogenic Ion Trap Vibrational Spectroscopy of Hydrogen-Bonded Clusters Relevant to Atmospheric Chemistry. *Int. Rev. Phys. Chem.* **2015**, *34*, 1−34.
(12) Shishido, R.; Kuo, J.-L.; Fujii, A. Structures and Dissociation Channels of Protonated Mixed Clusters around a Small Magic Number: Infrared Spectroscopy of $((CH_3)_3N)_n$-H^+-H_2O (n = 1−3). *J. Phys. Chem. A* **2012**, *116*, 6740−6749.
(13) Craig, S. M.; Menges, F. S.; Duong, C. H.; Denton, J. K.; Madison, L. R.; McCoy, A. B.; Johnson, M. A. Hidden Role of Intermolecular Proton Transfer in the Anomalously Diffuse Vibrational Spectrum of a Trapped Hydronium Ion. *Proc. Natl. Acad. Sci. U. S. A.* **2017**, *114*, E4706−E4713.
(14) Heine, N.; Kratz, E. G.; Bergmann, R.; Schofield, D. P.; Asmis, K. P.; Jordan, K. D.; McCoy, A. B. Vibrational Spectroscopy of the Water-Nitrate Complex in the O-H Stretching Region. *J. Phys. Chem. A* **2014**, *118*, 8188−8197.
(15) Henderson, B. V.; Jordan, K. D. One-Dimensional Adiabatic Model Approach for Calculating Progressions in Vibrational Spectra of Ion-Water Complexes. *J. Phys. Chem. A* **2019**, *123*, 7042−7050.
(16) Jiang, L.; Sun, S.-T.; Heine, N.; Liu, J.-W.; Yacovitch, T. I.; Wende, T.; Liu, Z.-F.; Neumark, D. M.; Asmis, K. R. Large Amplitude Motion in Cold Monohydrated Dihydrogen Phosphate Anions $H_2PO_4^-(H_2O)$: Infrared Photodissociation Spectroscopy Combined with Ab Initio Molecular Dynamics Simulations. *Phys. Chem. Chem. Phys.* **2014**, *16*, 1314−1318.
(17) Huang, Z. S.; Miller, R. E. High-Resolution near-Infrared Spectroscopy of Water Dimer. *J. Chem. Phys.* **1989**, *91*, 6613−6631.
(18) Tubergen, M. J.; Kuczkowski, R. L. Microwave Spectroscopic Characterization of a Strong Hydrogen Bond: Trimethylamine-Water. *J. Am. Chem. Soc.* **1993**, *115*, 9263−9266.
(19) Saykally, R. J.; Blake, G. A. Molecular Interactions and Hydrogen Bond Tunneling Dynamics: Some New Perspectives. *Science* **1993**, *259*, 1570−1575.
(20) Normile, D. Unique Free Electron Laser Laboratory Opens in China. *Science* **2017**, *355*, 235−235.
(21) Zhang, B.; et al. Infrared Spectroscopy of Neutral Water Dimer Based on a Tunable Vacuum Ultraviolet Free Electron Laser. *J. Phys. Chem. Lett.* **2020**, *11*, 851−855.
(22) Zhang, B.; et al. Infrared Spectroscopy of Neutral Water Clusters at Finite Temperature: Evidence for a Noncyclic Pentamer. *Proc. Natl. Acad. Sci. U. S. A.* **2020**, *117*, 15423−15428.
(23) Li, G.; et al. Infrared Spectroscopic Study of Hydrogen Bonding Topologies in the Smallest Ice Cube. *Nat. Commun.* **2020**, *11*, 5449.
(24) Hunter, E. P. L.; Lias, S. G. Evaluated Gas Phase Basicities and Proton Affinities of Molecules: An Update. *J. Phys. Chem. Ref. Data* **1998**, *27*, 413−656.
(25) Millen, D. J.; Zabicky, J. Hydrogen Bonding in Gaseous Mixtures: Amine-Alcohol Systems. *Nature* **1962**, *196*, 889−890.
(26) Ginn, S. G. W.; Wood, J. L. Hydrogen Bonding in Gaseous Mixtures: Amine-Alcohol Systems. *Nature* **1963**, *200*, 467−468.
(27) Carlson, G. L.; Witkowsk, Re; Fateley, W. G. Far Infra-Red Studies of Hydrogen Bonding in Gaseous Mixtures. *Nature* **1966**, *211*, 1289−1291.
(28) Millen, D. J.; Zabicky, J. Hydrogen Bonding in Gaseous Mixtures. Part V. Infrared Spectra of Amine-Alcohol Systems. *J. Chem. Soc.* **1965**, *0*, 3080−3085.
(29) Howard, D. L.; Kjaergaard, H. G. Vapor Phase Near Infrared Spectroscopy of the Hydrogen Bonded Methanol-Trimethylamine Complex. *J. Phys. Chem. A* **2006**, *110*, 9597−9601.
(30) Kjaersgaard, A.; Vogt, E.; Hansen, A. S.; Kjaergaard, H. G. Room Temperature Gas-Phase Detection and Gibbs Energies of Water Amine Bimolecular Complex Formation. *J. Phys. Chem. A* **2020**, *124*, 7113−7122.
(31) Ge, X.; Wexler, A. S.; Clegg, S. L. Atmospheric Amines - Part I. A Review. *Atmos. Environ.* **2011**, *45*, 524−546.
(32) von Schneidemesser, E.; et al. Chemistry and the Linkages between Air Quality and Climate Change. *Chem. Rev.* **2015**, *115*, 3856−3897.
(33) Yao, L.; et al. Atmospheric New Particle Formation from Sulfuric Acid and Amines in a Chinese Megacity. *Science* **2018**, *361*, 278−281.
(34) Even, U.; Jortner, J.; Noy, D.; Lavie, N.; Cossart-Magos, C. Cooling of Large Molecules below 1 K and He Clusters Formation. *J. Chem. Phys.* **2000**, *112*, 8068−8071.
(35) Huang, Q.-R.; Li, Y.-C.; Ho, K.-L.; Kuo, J.-L. Vibrational Spectra of Small Methylamine Clusters Accessed by an Ab Initio Anharmonic Approach. *Phys. Chem. Chem. Phys.* **2018**, *20*, 7653−7660.
(36) Zhang, B.; et al. Infrared Spectra of Neutral Dimethylamine Clusters: An Infrared-Vacuum Ultraviolet Spectroscopic and Anharmonic Vibrational Calculation Study. *J. Chem. Phys.* **2019**, *150*, No. 064317.
(37) Huang, Q.-R.; Endo, T.; Mishra, S.; Zhang, B.; Chen, L.-W.; Fujii, A.; Jiang, L.; Patwari, G. N.; Matsuda, Y.; Kuo, J.-L. Understanding Fermi Resonances in the Complex Vibrational Spectra of the Methyl Groups in Methylamines. *Phys. Chem. Chem. Phys.* **2021**, *23*, 3739.
(38) Sun, S.-T.; Jiang, L.; Liu, J. W.; Heine, N.; Yacovitch, T. I.; Wende, T.; Asmis, K. R.; Neumark, D. M.; Liu, Z.-F. Microhydrated Dihydrogen Phosphate Clusters Probed by Gas Phase Vibrational Spectroscopy and First Principles Calculations. *Phys. Chem. Chem. Phys.* **2015**, *17*, 25714−25724.
(39) Kong, X.; Sun, S.-T.; Jiang, L.; Liu, Z.-F. Solvation Effects on the Vibrational Modes in Hydrated Bicarbonate Clusters. *Phys. Chem. Chem. Phys.* **2018**, *20*, 4571−4578.
(40) Li, H.; Kong, X.; Jiang, L.; Liu, Z.-F. Solvation Effects on the N-O and O-H Stretching Modes in Hydrated $NO_3^-(H_2O)_n$ Clusters. *Phys. Chem. Chem. Phys.* **2018**, *20*, 26918−26925.
(41) Li, H.; Kong, X.; Jiang, L.; Liu, Z.-F. Size-Dependent Formation of an Ion Pair in $HSO_4^-(H_2O)_n$: A Molecular Model for Probing the Microsolvation of Acid Dissociation. *J. Phys. Chem. Lett.* **2019**, *10*, 2162−2169.
(42) VandeVondele, J.; Krack, M.; Mohamed, F.; Parrinello, M.; Chassaing, T.; Hutter, J. QUICKSTEP: Fast and Accurate Density Functional Calculations using a Mixed Gaussian and Plane Waves Approach. *Comput. Phys. Commun.* **2005**, *167*, 103−128.
(43) Barducci, A.; Bonomi, M.; Parrinello, M. Metadynamics. *Wiley Interdiscip. Rev.: Comput. Mol. Sci.* **2011**, *1*, 826−843.
(44) Tan, X. Q.; Ioannou, I. I.; Foltz, K. B.; Kuczkowski, R. L. The Methanol-Trimethylamine Complex: Structure and Large Amplitude Motions. *J. Mol. Spectrosc.* **1996**, *177*, 181−193.
(45) Shao, K.; Chen, J.; Zhao, Z.; Zhang, D. H. Communication: Fitting Potential Energy Surfaces with Fundamental Invariant Neural Network. *J. Chem. Phys.* **2016**, *145*, No. 071101.
(46) Chen, R.; Shao, K.; Fu, B.; Zhang, D. H. Fitting Potential Energy Surfaces with Fundamental Invariant Neural Network. II. Generating Fundamental Invariants for Molecular Systems with up to Ten Atoms. *J. Chem. Phys.* **2020**, *152*, 204307.
(47) Zhang, B.; Yang, S.; Huang, Q.-R.; Jiang, S.; Chen, R.; Yang, X.; Zhang, D. H.; Zhang, Z.; Kuo, J.-L.; Jiang, L. Deconstructing Vibrational Motions on the Potential Energy Surfaces of Hydrogen-Bonded Complexes. *CCS Chem.* **2021**, *3*, 829−835.
(48) Ho, K.-L.; Lee, L.-Y.; Katada, M.; Fujii, A.; Kuo, J.-L. An Ab Initio Anharmonic Approach to Study Vibrational Spectra of Small Ammonia Clusters. *Phys. Chem. Chem. Phys.* **2016**, *18*, 30498−30506.

https://dx.doi.org/10.1021/acs.jpclett.1c00168
J. Phys. Chem. Lett. 2021, 12, 2259−2265

(49) Huang, Q.-R.; Shishido, R.; Lin, C.-K.; Tsai, C.-W.; Tan, J. A.; Fujii, A.; Kuo, J.-L. Strong Fermi Resonance Associated with Proton Motions Revealed by Vibrational Spectra of Asymmetric Proton-Bound Dimers. *Angew. Chem., Int. Ed.* **2021**, *60*, 1936−1941.
(50) Buck, U.; Ettischer, I.; Melzer, M.; Buch, V.; Sadlej, J. Structure and Spectra of Three-Dimensional $(H_2O)_n$ Clusters, n = 8, 9, 10. *Phys. Rev. Lett.* **1998**, *80*, 2578−2581.
(51) Cole, W. T. S.; Farrell, J. D.; Wales, D. J.; Saykally, R. J. Structure and Torsional Dynamics of the Water Octamer from THz Laser Spectroscopy near 215 μm. *Science* **2016**, *352*, 1194−1197.

https://dx.doi.org/10.1021/acs.jpclett.1c00168
J. Phys. Chem. Lett. 2021, 12, 2259−2265